



Imperfect oriented attachment: Direct activation of high-temperature ferromagnetism in diluted magnetic semiconductor nanocrystals

Xuefeng Wang, J. B. Xu, Ning Ke, Jiaguo Yu, Juan Wang, Quan Li, H. C. Ong, and R. Zhang

Citation: [Applied Physics Letters](#) **88**, 223108 (2006); doi: 10.1063/1.2208554

View online: <http://dx.doi.org/10.1063/1.2208554>

View Table of Contents: <http://scitation.aip.org/content/aip/journal/apl/88/22?ver=pdfcov>

Published by the [AIP Publishing](#)

Articles you may be interested in

[Variation of structural and magnetic properties with Co-doping in \$\text{Zn}_{1-x}\text{Co}_x\text{O}\$ nanocrystals](#)

J. Appl. Phys. **105**, 053907 (2009); 10.1063/1.3087493

[Fabrication of Mn-doped ZnO diluted magnetic semiconductor nanostructures by chemical vapor deposition](#)

J. Appl. Phys. **99**, 08M119 (2006); 10.1063/1.2173235

[Synthesis and magnetic properties of \$\text{Zn}_{1-x}\text{Co}_x\text{O}\$ nanorods](#)

J. Appl. Phys. **99**, 074303 (2006); 10.1063/1.2188031

[Nanoscale magnet for semiconductor spintronics](#)

Appl. Phys. Lett. **88**, 122504 (2006); 10.1063/1.2186984

[Room-temperature ferromagnetic Co-doped ZnO nanoneedle array prepared by pulsed laser deposition](#)

Appl. Phys. Lett. **87**, 173119 (2005); 10.1063/1.2119415

The banner features the AIP Applied Physics Reviews logo on the left, which includes a small diagram of a device structure. The main text 'NEW Special Topic Sections' is in large, white, sans-serif font against a blue background with a glowing light effect. Below this, the text 'NOW ONLINE' is in yellow, followed by 'Lithium Niobate Properties and Applications: Reviews of Emerging Trends' in white. The AIP Applied Physics Reviews logo is repeated on the right side.

NEW Special Topic Sections

NOW ONLINE
Lithium Niobate Properties and Applications:
Reviews of Emerging Trends

AIP Applied Physics Reviews

Imperfect oriented attachment: Direct activation of high-temperature ferromagnetism in diluted magnetic semiconductor nanocrystals

Xuefeng Wang, J. B. Xu,^{a)} and Ning Ke

Department of Electronic Engineering, The Chinese University of Hong Kong, Shatin, New Territories, Hong Kong SAR, China

Jiaguo Yu

State Key Laboratory of Advanced Technology for Materials Synthesis and Processing, Wuhan University of Technology, Wuhan 430070, China

Juan Wang, Quan Li, and H. C. Ong

Department of Physics, The Chinese University of Hong Kong, Shatin, New Territories, Hong Kong SAR, China

R. Zhang

Department of Physics, Nanjing University, Nanjing 210093, China

(Received 8 December 2005; accepted 19 April 2006; published online 31 May 2006)

We report on a simple nonequilibrium solvothermal synthesis of Co-doped ZnO diluted magnetic semiconductor (DMS) nanocrystals. The crystal growth mechanism of imperfect three-dimensionally oriented attachment was revealed by the high-resolution transmission electron microscopy. The shallow donorlike defects as the legacy of aggregation-based growth were responsible for the observed high-temperature ferromagnetism (FM), further verifying the recent proposal. The solvothermal-treated strategy may not only offer an independent approach to directly tailor magnetic properties of advanced materials and devices at the nanoscale but also contribute to the sound understanding of the microscopic mechanism behind FM in DMSs. © 2006 American Institute of Physics. [DOI: 10.1063/1.2208554]

Nanostructured materials, acting as nanoscale building blocks, have been highly attractive in many disciplines.¹ Spontaneous self-assemblies of zero-dimensional nanoparticles (NPs) into higher-dimensional ordered architectures can significantly advance the understanding of novel electronic, magnetic, optical, transport, catalytic, and even biological properties.² Since the first exploration of self-assembled oriented attachment in the hydrothermal-treated anatase and iron oxyhydroxide nanocrystals by Banfield and co-workers,³ other examples have been clearly found in CuO,⁴ ZnO,⁵ and ZnS,⁶ demonstrating the self-orientation process of tiny NPs into highly ordered superstructures with/without surfactants. However, few have been demonstrated in the impurity-doped compound system.⁷ Controlled by the oriented attachment crystal growth mechanism, impurity incorporation is facile, as predicted by Alivisatos.⁸

Diluted magnetic semiconductors (DMSs) are of particular current interest since they are considered to be potentially suitable for future spintronics (spin-based electronics) applications.⁹ Among the various types of wide-band-gap semiconductors, ZnO has been one of the most promising host materials to realize new spintronic devices and magneto-optic components with high Curie temperature (T_C) after seamless integration of intrinsic ferromagnetism (FM).¹⁰ Indeed, ZnO doped with Mn,¹¹ Co,^{12,13} and Ni (Refs. 7 and 13) was found ferromagnetic at and above room temperature. However, to fully understand the latent microscopic magnetism is still of enormous challenges. In this regard, Kittilstved *et al.* have made significant progress, discovering a close link between the electronic structural origins and

polarity-dependent high- T_C FM in ZnO-based DMSs.¹⁴ Normally, anomalous Hall signal caused by free charge carriers is regarded as one of the direct manifestations of intrinsic FM.¹⁵ However, carrier-induced macroscopic conduction usually vanishes when the bound magnetic polaron (BMP) model¹⁶ is dominant, which suggests that the occurrence of high- T_C FM be attributed to the strong coupling between transition-metal (TM) impurities and localized charge carriers. Very recently, Gamelin and co-workers found that the origin of high- T_C FM is due to the shallow grain boundary defects created during aggregation/spin-coating/annealing process in ZnO,^{7,13} TiO₂,¹⁷ and SnO₂-based¹⁸ oxide DMSs.

In this letter, we report on a simple nonequilibrium solvothermal synthesis of a DMS, i.e., 5.6 at. % Co-doped ZnO nanocrystals (also denoted by CZO), through imperfect three-dimensionally oriented attachment mechanism. The vital importance of the shallow defects (electrons or holes) controlling FM proposed recently^{7,13–18} is further verified by the current independent solvothermal-treated strategy. Imperfect oriented attachment and high-temperature FM are therefore mutually correlated.

CZO samples were synthesized via a solvothermal technique from high-purity (Sigma Aldrich, over 99%) zinc acetate hydrate, cobalt acetate hydrate, and KOH using ethanol as a solvent without external surfactants in order to obviate the unnecessary contamination. The mixture was heated at around 190 °C for 24 h in an autoclave in the furnace, finally yielding a kind of blue powdery product. The Co dopant concentration was determined by inductively coupled plasma atomic emission spectrometry (Perkin-Elmer Optima 4300DV). Transmission electron microscopy (TEM) with high-resolution (HR) TEM imaging and electron energy-loss (EEL) elemental maps (FEI Tecnai 20 FEG operated at

^{a)}Electronic mail: jbxu@ee.cuhk.edu.hk

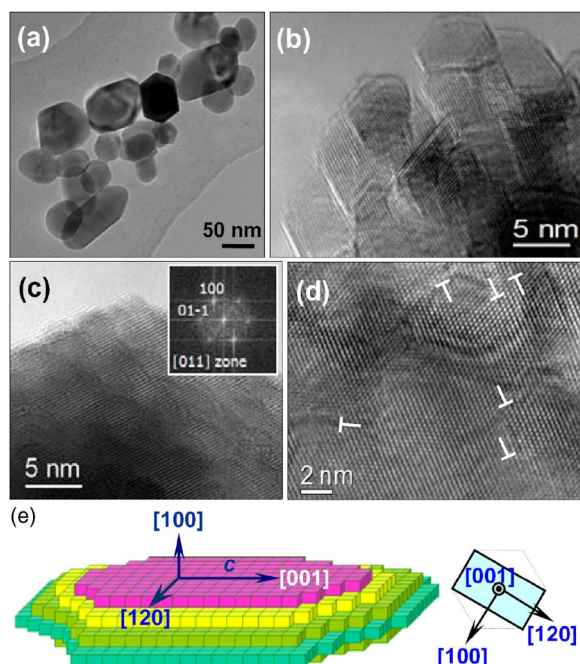


FIG. 1. (Color online) (a) A typical overview TEM image of CZO. (b) HRTEM image at the coarse edge of a NP. (c) HRTEM image at the peaked edge of a NP observed along the [011] zone axis. (d) HRTEM image of a NP containing many defects, indicating the imperfect oriented attachment mechanism. (e) Schematic illustration of ordered architecture of a matrix NP that is three-dimensionally aggregated from tiny NPs. It illustrates the origin of an obvious step surface viewed from the [011] zone axis by HRTEM in (c). Defects are inevitably created when lattice orientations slightly deviate from the perfect alignment among a number of tiny NPs (Ref. 3).

200 kV) was exploited to explore the underlying crystal growth mechanism. The magnetic properties were measured by a vibrating sample magnetometer (Oxford Instruments). Microcathodoluminescence (CL) was performed in a scanning electron microscope (Cambridge S360) equipped with a MonoCL system (Oxford Instruments). Hall-effect measurement was conducted using the four-point probe method at room temperature (Quantum Design PPMS).

An overview TEM image of CZO is shown in Fig. 1(a) with a broad size distribution. The average particle size is ca. 50 nm. Some NPs exhibit an elongation along a specific direction. Figure 1(b) illustrates the HRTEM image at the coarse edge of a NP, providing the clear evidence that the matrix NP is composed of many tiny nanosheets that are attached side by side with accordance of the lattice fringes. Therefore, it provides the preliminary indication of oriented attachment growth mechanism. Similar phenomenon was also observed in undoped ZnO nanorod and nanosheet-based hollow microhemispheres and microspheres.⁵ Noticeably, as shown in Fig. 1(c), the contrast of HRTEM image at the peaked edge of a NP appears like a terrace associated with steps along the [011] zone axis, further indicating that the matrix NP consists of numerous tiny NPs. They are attached side by side along the same directions. The accordance of the corresponding fast Fourier transforms [Fig. 1(c) inset] from different areas of the matrix NP demonstrates that the matrix NP is single crystalline, corroborating the oriented attachment growth mechanism. The structural defects such as edge dislocations, stacking faults, and lattice distortions can be easily found in some regions of the matrix NP [Fig. 1(d)], characteristic of the imperfect oriented attachment.³ A typical three-dimensionally ordered architecture of a matrix NP is

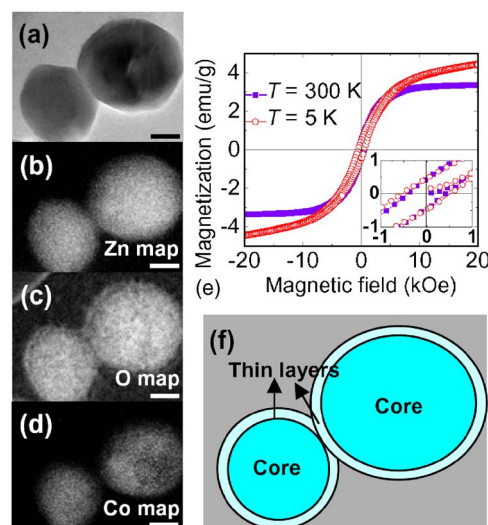


FIG. 2. (Color online) Typical EEL elemental maps and magnetization of CZO. Scale bars=20 nm. (a) Original TEM image of two adjacent NPs. [(b)-(d)] Elemental maps of Zn, O, and Co elements, respectively. (e) Hysteresis loops measured at 5 and 300 K. The inset shows the enlargement of the hysteresis loops near the origin, showing the coercivity (H_C) of about 520 and 420 Oe at 5 and 300 K, respectively. (f) Schematic illustration of a core-shell structural model of two adjacent NPs shown in (a).

schematically shown in Fig. 1(e). We state that the presence of counterions (acetate anions and OH^-) in the solvothermal-solution system plays an important role in preventing NPs from diffusing and the faster preferential growth along the [001] direction, thus resulting in the nearly round NPs with a broad size distribution [Fig. 1(a)].

Figures 2(b)–2(d) show the typical EEL elemental maps of two adjacent NPs [see Fig. 2(a)], providing a direct evidence of successful impurity doping into the host. Elemental maps indicate a relatively homogeneous distribution of Zn, O, and Co elements in the matrix NPs except in the thin surface layers. The smaller region of Co map in Fig. 2(d) is qualitatively due to the smaller Co concentration in the thin surface layers. Thus, the magnetic properties of thin surface layers of NPs are expected to be strikingly different from those of cores. Figure 2(e) shows the well-defined hysteresis loops of CZO at 5 and 300 K, indicating its robust ferromagnetic nature with high T_C (>300 K). However, at low temperature (5 K), CZO is hard to saturate magnetically, and the loop contains paramagnetic part. This is ascribed to the weakly coupled Co^{2+} ions largely located in the thin surface layers. Directly inferred from Fig. 2(d), these NPs are composed of ferromagnetic cores and surrounding paramagnetic shells, as schematically shown in Fig. 2(f). This is consistent with the previous proposal of the core-shell model (ferromagnetic domains surrounded by paramagnetic TM ions) derived from the temperature-dependent coercivity (associated with an activation barrier) in Ni-doped ZnO aggregates.⁷

Moreover, defects induced by imperfect oriented aggregation-based growth can be found in the preliminary CL spectrum at room temperature (Fig. 3). The 3.18 eV UV emission is attributed to the near-band-edge (NBE) transition from the recombination of free excitons. Doping is believed to exacerbate the imperfect oriented attachment and hence activates the intense and broad green (2.37 eV) emission band. It is reasonable that the green emission is ascribed to the defect-level (DL) emission involving the shallow donor electrons which are likely doubly occupied oxygen vacancies

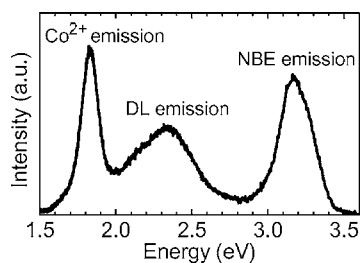


FIG. 3. Room-temperature CL spectrum of CZO.

and/or zinc interstitials.^{16,19} Remarkably, a sharp red band emission centered at ca. 1.83 eV (678 nm) is observed, which is due to the ${}^4T_1(P) \rightarrow {}^4A_2(F)$ $d-d$ radiative transition of the internal Co^{2+} ions in a tetrahedral crystal field.²⁰ Co^{2+} -ion emission at about 1.8 eV in ZnO (Ref. 20) and other TM-ion emission in other semiconductors²¹ have been also observed, while the disappearance of TM-ion emission^{11,13} may be due to the nonradiative recombination process by the surface traps or other potential quenchers.²²

Hall-effect measurement shows the relatively large resistance of CZO at room temperature ($>10^7 \Omega \text{ cm}$, which is beyond the measurement range). Hence, we clarify the origin of FM in the basic framework of the BMP model,¹⁶ in which the itinerant shallow donor electrons are strongly hybridized with the localized unfilled $3d^4$ orbitals of Co dopant to yield BMPs with effective Bohr orbital radii of about 0.76 nm.¹⁶ The BMPs tend to overlap and create a spin-split impurity band at the Fermi level in the forbidden band, hence leading to high- T_C FM. If the donor level is deep, it is difficult to significantly affect the occupancy of the extended Co^{2+} level. In our case we cannot rule out the existence of deep donors such as singly occupied oxygen vacancies. Therefore, we can also attribute the unsuccessful ferromagnetic coupling of Co^{2+} ions located in the thin surface layers of NPs to the absence of effective shallow donors. Normally, the absence of FM in TM-doped ZnO under the high-temperature processing conditions^{23,24} is due to the fact that the shallow defects are generally eliminated upon the high-temperature treatment.

Finally, we point out that the solvothermal-treated crystal growth mechanism (imperfect oriented attachment) is similar to the reaction-limited aggregation from quantum dots under an isocrystalline core/shell procedure.⁷ Hence, the role of shallow donor defects induced here is identical with that of shallow grain boundary defects induced before under appropriate conditions.^{7,13,17,18}

In summary, we have demonstrated that the observed high- T_C FM in a DMS (the ternary Co–Zn–O system) is closely linked to the crystal growth mechanism, i.e., the imperfect three-dimensionally oriented attachment via a simple

solvothermal-treated strategy. Shallow bound-donor defects, which are the legacy of imperfect oriented aggregation-based growth, form the strongly coupled BMPs with $3d^4$ orbitals of substitutional Co in NP cores, hence leading to high- T_C FM. The solvothermal-treated strategy demonstrated here may provide a new bottom-up avenue to the realization of more complex ferromagnetic nanostructured spintronic materials and devices.

The authors thank J. An, B. Zhang, and Professor X. X. Zhang for useful discussions and Dr. W. Y. Cheung and W. K. Chan for technical assistance. Financial support from CUHK and RGC of HKSAR is gratefully acknowledged.

¹M. Li, H. Schnablegger, and S. Mann, *Nature (London)* **402**, 393 (1999); Y. Yin and A. P. Alivisatos, *ibid.* **437**, 664 (2005).

²Z. Tang and N. A. Kotov, *Adv. Mater. (Weinheim, Ger.)* **17**, 951 (2005).

³R. L. Penn and J. F. Banfield, *Science* **281**, 969 (1998); J. F. Banfield, S. A. Welch, H. Zhang, T. T. Ebert, and R. L. Penn, *ibid.* **289**, 751 (2000).

⁴Z. Zhang, H. Sun, X. Shao, D. Li, H. Yu, and M. Han, *Adv. Mater. (Weinheim, Ger.)* **17**, 42 (2005).

⁵M. Mo, J. C. Yu, L. Zhang, and S.-K. A. Li, *Adv. Mater. (Weinheim, Ger.)* **17**, 756 (2005).

⁶F. Huang, H. Zhang, and J. F. Banfield, *Nano Lett.* **3**, 373 (2003).

⁷P. V. Radovanovic and D. R. Gamelin, *Phys. Rev. Lett.* **91**, 157202 (2003).

⁸A. P. Alivisatos, *Science* **289**, 736 (2000).

⁹H. Ohno, *Science* **281**, 951 (1998); S. A. Wolf, D. D. Awschalom, R. A. Buhrman, J. M. Daughton, S. von Molnar, M. L. Roukes, A. Y. Chhetkanova, and D. M. Treger, *ibid.* **294**, 1488 (2001).

¹⁰S. J. Pearton, D. P. Norton, K. Ip, Y. W. Heo, and T. Steiner, *Prog. Mater. Sci.* **50**, 293 (2005).

¹¹J. M. Baik and J.-L. Lee, *Adv. Mater. (Weinheim, Ger.)* **17**, 2745 (2005).

¹²J. J. Chen, M. H. Yu, W. L. Zhou, K. Sun, and L. M. Wang, *Appl. Phys. Lett.* **87**, 173119 (2005).

¹³D. A. Schwartz, N. S. Norberg, Q. P. Nguyen, J. M. Parker, and D. R. Gamelin, *J. Am. Chem. Soc.* **125**, 13205 (2003).

¹⁴K. R. Kittilstved, W. K. Liu, and D. R. Gamelin, *Nat. Mater.* **5**, 291 (2006).

¹⁵H. Toyosaki, T. Fukumura, Y. Yamada, K. Nakajima, T. Chikyow, T. Hasegawa, H. Koinuma, and M. Kawasaki, *Nat. Mater.* **3**, 221 (2004).

¹⁶J. M. D. Coey, M. Venkatesan, and C. B. Fitzgerald, *Nat. Mater.* **4**, 173 (2005).

¹⁷J. D. Bryan, S. A. Santangelo, S. C. Keveren, and D. R. Gamelin, *J. Am. Chem. Soc.* **127**, 15568 (2005).

¹⁸P. I. Archer, P. V. Radovanovic, S. M. Heald, and D. R. Gamelin, *J. Am. Chem. Soc.* **127**, 14479 (2005).

¹⁹S. B. Zhang, S. H. Wei, and A. Zunger, *Phys. Rev. B* **63**, 075205 (2001).

²⁰P. Lommens, P. F. Smet, C. de Mello Donega, A. Meijerink, L. Piraux, S. Michotte, S. Matefi-Tempfli, D. Poelman, and Z. Hens, *J. Lumin.* **118**, 245 (2006); B. D. Yuhas, D. O. Zitoun, P. J. Pauzauskie, R. He, and P. Yang, *Angew. Chem., Int. Ed.* **45**, 420 (2006).

²¹W. Chen, J. Z. Zhang, and A. G. Joly, *J. Nanosci. Nanotechnol.* **4**, 919 (2004).

²²M. H. Ullah and C.-S. Ha, *J. Nanosci. Nanotechnol.* **5**, 1376 (2005).

²³C. N. R. Rao and F. L. Deepak, *J. Mater. Chem.* **15**, 573 (2005).

²⁴G. Lawes, A. S. Risbud, A. P. Ramirez, and R. Seshadri, *Phys. Rev. B* **71**, 045201 (2005).